

Search for Quasi-Periodical Oscillations in Precursors of Short and Long Gamma Ray Bursts

SHUO XIAO,^{1,2} WEN-XI PENG*,³ SHUANG-NAN ZHANG*,³ SHAO-LIN XIONG*,³ XIAO-BO LI,³ YOU-LI TUO,³ HE GAO,⁴
YUE WANG,^{3,5} WANG-CHEN XUE,^{3,5} CHAO ZHENG,^{3,5} YAN-QIU ZHANG,^{3,5} JIA-CONG LIU,^{3,5} CHENG-KUI LI,³ SHU-XU YI,³
XI-LU WANG,³ ZHEN ZHANG,³ CE CAI,⁶ AI-JUN DONG,^{1,2} WEI XIE,^{1,2} JIAN-CHAO FENG,^{1,2} QING-BO MA,^{1,2} DE-HUA WANG,^{1,2}
XI-HONG LUO,^{1,2} QI-JUN ZHI,^{1,2} LI-MING SONG,³ AND TI-PEI LI^{3,7}

¹Guizhou Provincial Key Laboratory of Radio Astronomy and Data Processing, Guizhou Normal University, Guiyang 550001, People's Republic of China

²School of Physics and Electronic Science, Guizhou Normal University, Guiyang 550001, People's Republic of China

³Key Laboratory of Particle Astrophysics, Institute of High Energy Physics, Chinese Academy of Sciences, Beijing 100049, China

⁴Department of Astronomy, Beijing Normal University, Beijing 100875, People's Republic of China

⁵University of Chinese Academy of Sciences, Chinese Academy of Sciences, Beijing 100049, China

⁶College of Physics, Hebei Normal University, 20 South Erhuan Road, Shijiazhuang, 050024, China

⁷Department of Astronomy, Tsinghua University, Beijing 100084, People's Republic of China

ABSTRACT

The precursors of short and long Gamma Ray Bursts (SGRBs and LGRBs) can serve as probes of their progenitors, as well as shedding light on the physical processes of mergers or core-collapse supernovae. Some models predict the possible existence of Quasi-Periodically Oscillations (QPO) in the precursors of SGRBs. Although many previous studies have performed QPO search in the main emission of SGRBs and LGRBs, so far there was no systematic QPO search in their precursors. In this work, we perform a detailed QPO search in the precursors of SGRBs and LGRBs detected by Fermi/GBM from 2008 to 2019 using the power density spectrum (PDS) in frequency domain and Gaussian processes (GP) in time domain. We do not find any convinced QPO signal with significance above 3σ , possibly due to the low fluxes of precursors. Finally, the PDS continuum properties of both the precursors and main emissions are also studied for the first time, and no significant difference is found in the distributions of the PDS slope for precursors and main emissions in both SGRBs and LGRBs.

Keywords: gamma ray bursts – methods: data analysis

1. INTRODUCTION

Gamma-Ray Bursts (GRBs) are traditionally divided into long GRBs (LGRBs) and short GRBs (SGRBs) based on their duration (separated at about 2 s). LGRBs are widely believed to originate from core collapses of massive stars and associated with supernovae, whereas SGRBs are related to binary neutron star or neutron star-black hole mergers (Woosley & Bloom 2006; Abbott et al. 2017) where a kilonova due to a series of r-process nucleosynthesis (Li & Paczyński 1998; Wu et al. 2017) can be seen. Precursors are detected in about 10% of GRBs detected by Swift and most of them are LGRBs, and no significant difference was found between the precursor emission and the main emission episodes, suggesting that the precursors are directly related to the central engine activities and thus share the same physical origin with

the prompt episode (Hu et al. 2014; Li & Mao 2022). A few SGRBs, about 2.7% of SGRBs detected by Swift/BAT and Fermi/GBM, also have precursor emission, which usually have a blackbody or exponential cutoff power-law (CPL) spectra (Zhong et al. 2019; Wang et al. 2020). The thermal precursor of SGRB may originate from the shock breakout or the photospheric radiation of a fireball launched after the merger, whereas nonthermal precursors may be explained by magnetospheric interaction between two neutron stars prior to the merger (Hansen & Lyutikov 2001; Troja et al. 2010; Palenzuela et al. 2013; Wang et al. 2018), or the the resonant shattering of the crusts of neutron star (Tsang et al. 2012).

Many previous studies have performed QPO search in main emission of SGRBs (e.g Kruger et al. 2002; Zhilyaev & Dubinovska 2009; Dichiara et al. 2013) and LGRBs (e.g. Kruger et al. 2002; Cenko et al. 2010; Guidorzi et al. 2016; Tarnopolski & Marchenko 2021), where the former may originate from quasi-periodic jet precession from black hole (BH)–neutron star (NS) mergers (Stone et al. 2013), and the latter may be related to the long activity of the magne-

tars (Markwardt et al. 2009). However, none of the claimed QPOs has been confirmed by further studies.

On the other hand, some models predict the possible existence of QPOs in precursors of SGRBs, such as pre-merger magnetosphere interaction (Xiao et al. 2022a), magnetar tidal-induced super flare model (Zhang et al. 2022), seismic aftershocks from resonant scattering of neutron star (Sarin & Lasky 2021; Suvorov et al. 2022) and the accelerating relativistic binary winds via the synchrotron maser process (Sridhar et al. 2021). Indeed, recently a Quasi-Periodic oscillations (QPOs) has been reported in the non-thermal precursor of GRB 211211A (Xiao et al. 2022a). This GRB lasts for about 50 seconds (Mangan et al. 2021); however, a kilonova was detected (Rastinejad et al. 2022; Xiao et al. 2022a) accompanying the GRB, and its spectral lag is only several milliseconds, consistent with that of SGRB (Xiao et al. 2022b; Troja et al. 2022). Besides, its positions on the spectral Lag - luminosity ($L_{\text{ag}} - L_{\text{iso}}$) and Amati diagrams are consistent with the merger origin (Xiao et al. 2022a; Rastinejad et al. 2022; Yang et al. 2022). This QPO may be generated by the torsional or crustal oscillations of the magnetar (Xiao et al. 2022a; Gao et al. 2022; Suvorov et al. 2022; Zhang et al. 2022).

However, so far there was no systematic QPO search in the precursors of both SGRBs and LGRBs, which is the focus of this work. We present our sample selection and search methods in Section 2, and give the results in Section 3. Finally, discussion and summary are given in Section 4.

2. SAMPLE SELECTION AND METHODOLOGY

2.1. Data selection

A precursor usually should satisfy the following requirements (Troja et al. 2010; Wang et al. 2020): (1) the first pulse in the GRB; (2) the peak count rate is lower than that of the main pulse; (3) the count rate during the waiting time period is consistent with the background level. We collect our samples for SGRBs and LGRBs with precursors observed by GBM from literature (Burlon et al. 2008; Hu et al. 2014; Minaev & Pozanenko 2017; Zhong et al. 2019; Coppin et al. 2020; Wang et al. 2020; Li & Mao 2022). From 2008 to 2019, there are 24 samples of precursors for SGRBs (see Table 1) and 185 samples for LGRBs precursor.

To improve the statistics, only those detectors of GBM for which the incident angle of the source is less than 90 degrees for SGRBs and 70 degrees for LGRBs are selected, and only the events in the energy range 8-900 keV are used in this analysis. It is worth noting that since most of GRBs are not precisely located, and especially for SGRBs with large localization errors, we use the GRB direction with the highest probability (i.e. central value) as a reference for detector selection.

2.2. Significance of the precursors

Since the QPO search depends on the brightness of the signal (i.e. signal-to-noise ratio) (e.g. Lewin et al. 1988), we calculate the significance of the candidate precursor signal by Li-Ma formula (Li & Ma 1983), which is defined as

$$S = \sqrt{2} \left\{ n \log \left[\frac{\alpha + 1}{\alpha} \left(\frac{n}{n + b} \right) \right] + b \log \left[(\alpha + 1) \frac{b}{n + b} \right] \right\}^{1/2}, \quad (1)$$

where n is the counts of a certain time t_{on} within which a suspected source exists, b is the measured background counts in a time interval t_{off} , and α is the ratio of the on-source time to the off-source time $t_{\text{on}}/t_{\text{off}}$.

On the other hand, dead time has an intricate effect on the periodogram (Huppenkothen et al. 2013). Fortunately, the dead time of a single normal event of GBM is only 2.6 μs (Meegan et al. 2009), and there are no extremely bright or saturated ones in our precursor sample, therefore the effect of dead time does not need to be considered in this work.

2.3. Search for periodic signals

Most common methods for QPOs search are frequency-domain based methods such as periodograms or power spectra, which are based on assumption that bins in a periodogram are χ_2^2 -distributed, thus a Whittle likelihood applies. It is only strictly true for infinitely long time series with homoscedastic stationary Gaussian data (Hübner et al. 2022b); however, for fast transients like GRBs, the statistical distributions at low frequencies are not stationary processes (Huppenkothen et al. 2013; Hübner et al. 2022a). Recently, Hübner et al. proposed to search for QPOs in astrophysical transients based on Gaussian processes (GP) (Hübner et al. 2022b), which can investigate QPO directly in the time domain and take account of heteroscedasticity and non-stationarity in data. Here we use both methods, i.e., Power density spectrum (PDS) and Gaussian processes, to search for the QPO frequency from about 1 to 1000 Hz and to estimate the significance of the possible QPOs. Since the precursor of a SGRB usually has only one FRED-shaped pulse, both methods can be applied. However, the precursor of a LGRB usually has several pulses, thus we do not use the GP method for LGRBs.

2.3.1. Power density spectrum method

Within a Bayesian framework, we model the periodogram as a combination of red noise at low frequencies and white noise at high frequencies with a power-law plus a constant (Vaughan 2010; Guidorzi et al. 2016; Huppenkothen et al. 2013),

$$S_{\text{plc}}(f) = \beta f^{-\alpha} + \gamma. \quad (2)$$

When we have a parametric power spectral model with known parameters θ , $S_j(\theta)$, the ratio (or residuals) $R_j^{\text{obj}} =$

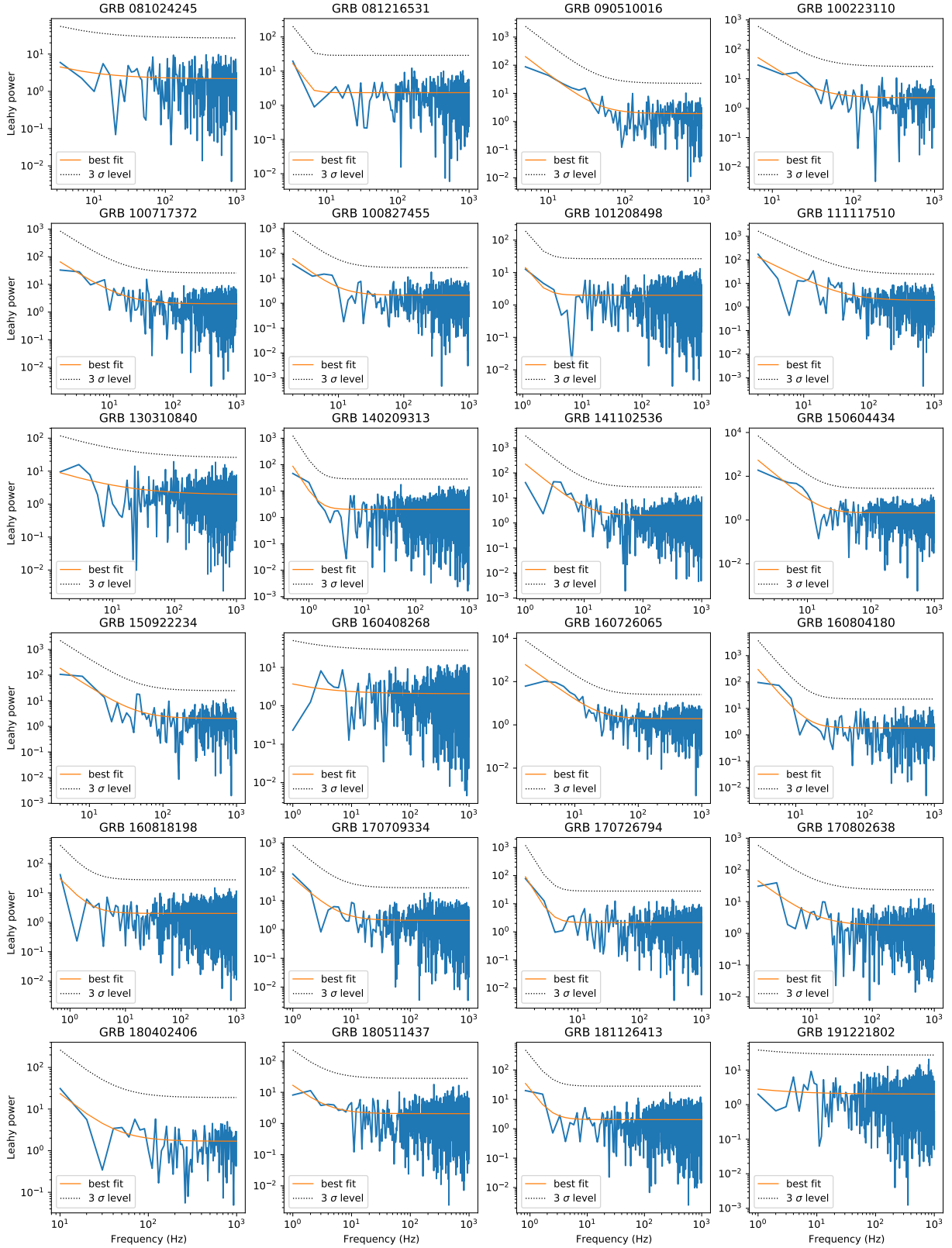


Figure 1. PDS of precursors in SGRBs. The solid orange lines show the best-fitting power law+constant models, and the black dotted lines represent the 3σ level. The number of frequencies searched is corrected.

Table 1. QPOs search for precursors in SGRBs using Power density spectrum and Gaussian processes methods.

Name ^a	T _{pre} (s)	Li-Ma Significance ^b (σ)	f_{PDS} (Hz)	$p_{\text{value}}(\text{PDS})$	f_{GP} (Hz)	$\ln BF_{\text{qpo}}(\text{GP})^c$
GRB 081024245	0.06	1.9	556	0.98	475	-1.9
GRB 081216531	0.15	4.1	156	0.86	174	0.3
GRB 090510016	0.05	5.7	621	0.53	119	0.2
GRB 100223110	0.02	3.5	226	0.74	226	0.2
GRB 100717372	0.15	7.6	38	0.79	301	-1.0
GRB 100827455	0.11	3.7	264	0.1	144	-0.5
GRB 101208498	0.17	7.1	939	0.7	429	-0.2
GRB 111117510	0.18	13.7	358	0.81	287	-0.2
GRB 130310840	0.58	2.6	458	0.06	459	-3.2
GRB 140209313	0.61	7.1	53	0.29	8	1.0
GRB 141102536	0.06	5.0	362	0.32	302	0.9
GRB 150604434	0.17	9.5	884	0.6	499	-0.4
GRB 150922234	0.05	9.2	709	0.56	341	-2.0
GRB 160408268	0.07	0.1	627	0.98	317	-1.9
GRB 160726065	0.08	6.5	276	0.85	247	-0.2
GRB 160804180	0.16	10.3	357	0.33	358	-1.6
GRB 160818198	0.6	8.3	407	0.57	13	-0.8
GRB 170709334	0.46	6.6	219	0.1	302	0.5
GRB 170726794	0.28	9.1	337	0.59	418	-0.3
GRB 170802638	0.15	4.6	700	0.39	98	-1.1
GRB 180402406	0.03	5.9	120	0.99	249	-1.0
GRB 180511437	2.80	1.2	252	0.17	468	0.1
GRB 181126413	0.72	4.1	277	0.3	220	-1.6
GRB 191221802	0.03	1.0	806	0.05	140	-1.8

^a The samples and T_{pre} (i.e. the duration of precursor) are from [Zhong et al. 2019](#) and [Wang et al. 2020](#).^b Significance of the signal of precursor obtained from the Li-Ma formula ([Li & Ma 1983](#)).^c BF_{qpo} is the Bayes factor, the $\ln BF_{\text{qpo}}(\text{GP})=3$ corresponds approximately to a p -value of 0.001 ([Hübner et al. 2022b](#)).

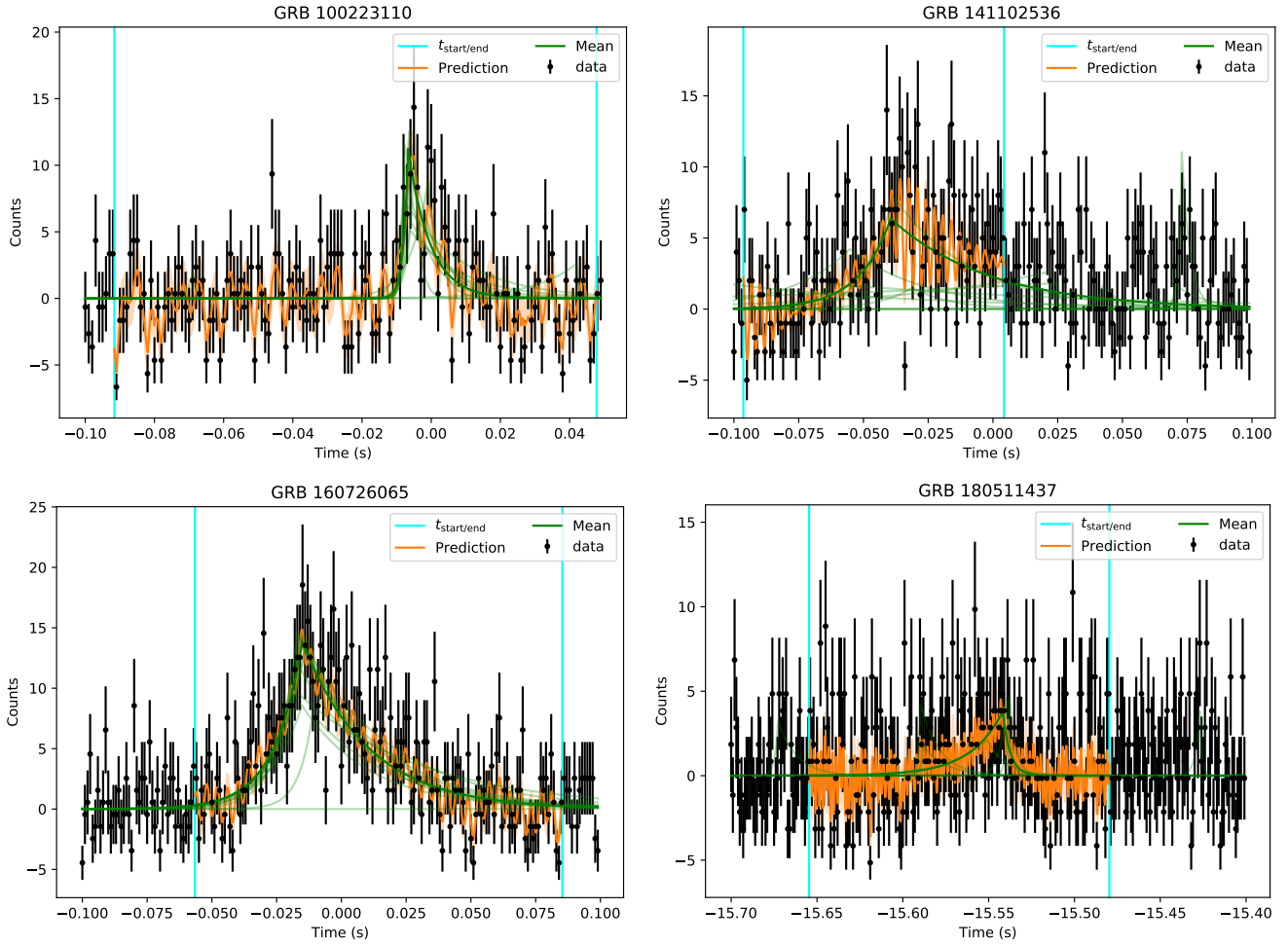


Figure 2. The light curves of precursors in GRB 100223110, GRB 141102536, GRB 160726065 and GRB 180511437. The green lines are the mean functions (i.e. FRED) from the maximum likelihood samples, the orange lines are the predictions based on the maximum likelihood samples, and the light blue vertical lines are the maximum likelihood start or end of the red noise and possible QPO. However, the $\ln BF_{\text{QPO}}$ of them are all less than 3, that is, there is not enough significance to confirm the existence of QPO. The time bin size of light curves are 1 ms.

$2I_j^{\text{obs}}/S_j(\theta)$ will follow a χ_v^2 distribution with $v = 2$ degrees of freedom (Vaughan 2005), and the highest outlier in the residuals is the candidate QPO.

To estimate the p -value (or significance), we simulate a large number of periodograms from the sample of Markov Chain Monte Carlo simulations (MCMC), compute the residuals and find the maximum outlier in the residuals for each periodogram. Finally, we calculate the p -value of the maximum outlier of the real burst in the distribution of maximum outliers from the set of simulations derived from the broadband noise model with no periodicity (see Huppenkothen et al. 2013 for details). We perform some of the above calculations using *Stingray* package¹ (Huppenkothen et al. 2019). It is worth noting that the most conservative correction for the number of trials should be applied, that is, the

¹ <https://docs.stingray.science/index.html>

p -values are corrected for the number of bursts searched and frequencies searched. However for the purpose of comparing the results of SGRBs and LGRBs, the significance reported in Table 1 is only corrected for the number of frequencies searched but not for the number of bursts searched. To achieve a frequency search up to 1000 Hz, the time bin size of the light curves is 0.5 ms.

2.3.2. Gaussian processes

We adopt the procedure in Hübner et al. 2022b. It models QPOs as a stochastic process on top of a deterministic shape (i.e. mean function). For the deterministic shape, we find that a FRED can be better fitted to the precursors of SGRBs. For the stochastic process, we define the kernels describing a periodic oscillation and red noise as follows,

$$\begin{aligned} k_{\text{qpo}}(\tau) &= a_0 \cos(2\pi f\tau) \exp(-c_0\tau), \\ k_{\text{rn}}(\tau) &= a_1 \exp(-c_1\tau), \end{aligned} \quad (3)$$

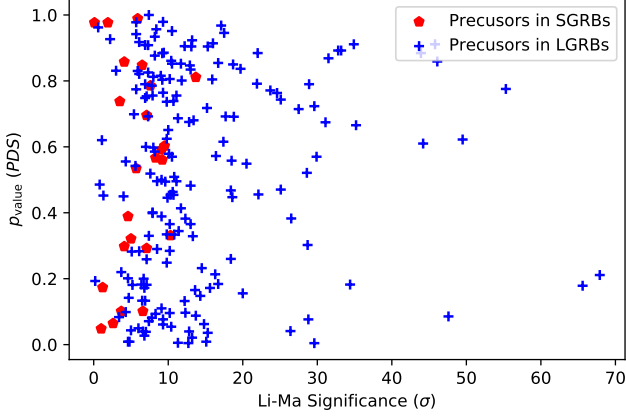


Figure 3. The Li-Ma significance versus the p_{value} (PDS) of potential QPO. The Pearson correlation coefficients for them are 0.17 and 0.08 for precursors of SGRBs and LGRBs, respectively. Thus no clues are found for the common presence of QPO in the precursors.

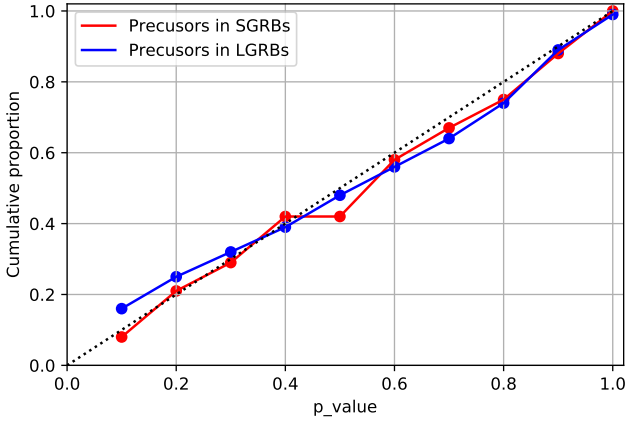


Figure 4. p -value region versus the fraction of times that the p -value falls within $\leq p$ -value for PDS method. The black dotted line represents the perfect one-to-one relation.

where a_0 is the amplitude of the oscillation at frequency f , c_0 a description of the decay of the QPO with time constant τ , a_1 , and c_1 are the amplitude of red noise and the decay with time, respectively.

To assess the significance of the QPO, we perform model selection between QPOs and red noise (for more detailed information refer to Hübner et al. (2022b)), the Bayes factor BF_{qpo} is defined as

$$BF_{\text{qpo}} = \frac{Z(d|k_{\text{qpo}+\text{rn}}, \mu)}{Z(d|k_{\text{rn}}, \mu)}, \quad (4)$$

where $Z(d|k_{\text{qpo}+\text{rn}}, \mu)$ (i.e. QPO and red noise) and $Z(d|k_{\text{rn}}, \mu)$ (i.e. red noise) are the respective evidence in the different models, the μ is the parameter of the mean function and d represents data. Finally, Z is the evidence describing

the overall probability that a given model for data,

$$Z(d|S) = \int \pi(\theta)L(d|\theta, S)d\theta, \quad (5)$$

$$L(d|\theta, M) = \frac{p(\theta|d, M)Z(d|M)}{\pi(\theta|M)},$$

where θ , d , M and $p(\theta|d, M)$ are parameters, data, model and the posterior probability, respectively; $\pi(\theta|M)$ and $L(d|\theta, M)$ are the *prior* probability and likelihood, respectively.

To improve the statistics (i.e. the statistical fluctuation in counts is large when the time bin size is too small), the time bin size of the light curves is set as 1 ms, which a frequency search up to 500 Hz. When $\ln BF_{\text{qpo}} > 3$, it is very unlikely that we have seen a false positive, which corresponds to a p -value of approximately 0.001 (see Fig. 5 in Hübner et al. 2022b). In this work, we refer to the publicly available code of GP² released by Hübner et al. 2022b and report the result in this work using non-stationary models.

3. RESULT

3.1. Precursors in SGRBs

We search for QPOs for the 24 SGRBs precursors using both the PDS and GP methods, and the results are shown in Table 1, note we only report the frequency with the highest deviation (i.e. minimum p -value) from the best fit model for that specific power density spectra. We found no candidate with significance above 3σ or $\ln BF_{\text{qpo}} > 3$. However, it is worth noting that we cannot exclude the possibility of the existence of QPOs in SGRBs precursors, as most of them are very weak (i.e. a few net counts). The Pearson correlation coefficient (see Fig. 3) for the Li-Ma significance and p -value of potential QPO is 0.17 (smaller negative values represent higher significance of potential common QPO for precursors, that is, brighter precursors should have smaller p -values (or higher significance)), i.e., no clues are found for the common presence of QPOs in the precursors of SGRBs.

For the results obtained by the GP method, although all $\ln BF_{\text{qpo}}$ are less than 3 (i.e. $< 3\sigma$), we note that some candidate QPO frequencies are consistent with the results obtained in the PDS (e.g. GRB 100223110). In Fig. 2, we show the light curves of four precursors for which the GP model fits the data relatively well; however, it is difficult to confirm the existence of QPOs due to the low statistics.

3.2. Precursors in LGRBs

In contrast to SGRBs, most precursors in LGRBs have sufficient net counts to test whether QPOs really exist. We search for QPOs for the 185 LGRB precursors using PDS,

² <https://github.com/MoritzThomasHuebner/QPOEstimation>

but also find no candidate with significance above 3σ . The Pearson correlation coefficient for the Li-Ma significance and p -value of potential QPO is 0.08 (see Fig. 3), and thus no clues are found for the common presence of QPO in the precursors of LGRBs.

In order to verify the robustness of the p -value estimation in PDS method (in the Tabel. S1), that is, whether the percentage of samples smaller than a certain p -value is this p -value, assuming that QPOs do not commonly exist. As shown by the blue solid line in Fig. 4 (or the cumulative distribution of p -values obtained for best QPO candidate of each precursor), each quoted p -value contains samples with a percentage close to its nominal level, which means that the p -value estimation is robust. In addition, the p -value estimation of QPOs for SGRB precursors (in the Tabel. 1) is also robust (see red solid line in Fig. 4).

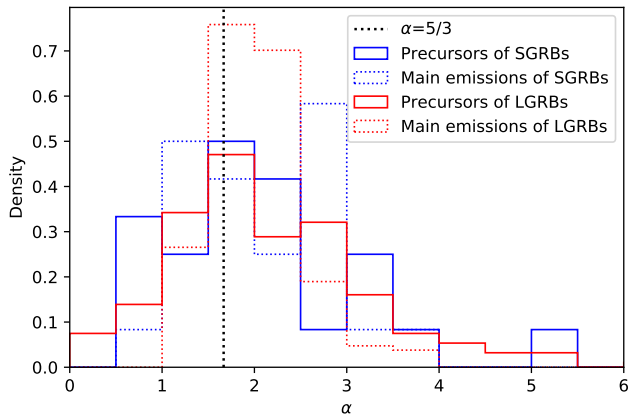


Figure 5. Distribution of the PDS slope (α) for precursors and main emissions of SGRBs and LGRBs.

4. DISCUSSION AND CONCLUSION

We do not find any convinced QPO signal (with significance $> 3\sigma$) in the precursors of SGRBs and LGRBs observed by GBM from 2008 to 2019 based on the frequency-domain (i.e. PDS) and time-domain (i.e. GP) methods. We can rule out the possibility that QPOs commonly exist in LGRB precursors with their large sample and sufficient brightness. However, our results do not allow us to exclude the possibility of the common QPO existence in SGRB precursors due to their relatively small sample and weak signal.

The Li-Ma significance levels of the individual precursors of SGRBs (e.g. GRB 160408268) are very low with the GBM data due to a few counts; these precursors were detected relatively significantly only by Swift/BAT. Besides, we classify LGRBs and SGRBs in this work only with their duration; however, since the ‘tip-of-iceberg’ effect (Lü et al. 2014) may make what would have been a long burst to be observed as a SGRB with a precursor. Further studies should

classify GRBs by spectral lag and spectral shape, for example, SGRBs are commonly associated with harder spectra and spectral lags consistent with ~ 0 s (Berger 2014). In addition, we also find that in some of the light curves of individual samples taken from the literature the count rates in waiting times are not strictly the same as the background level, such as GRB 150922234 and GRB 160804180 (see Wang et al. 2020), that is, some SGRB precursors may be also LGRBs. The above two factors means that the real sample of SGRBs may be even smaller.

The lack of unambiguous evidence for QPO signal in the precursors of LGRBs does not conflict with the precursor model, in which the precursor is considered to be directly related to the central engine activities and shares the same physical origin with the prompt episode (Hu et al. 2014). This is consistent with the fact that no confirmed candidates are found in the previous QPO searches in the main emissions of LGRBs (Dichiara et al. 2013; Huppenkothen et al. 2013; Guidorzi et al. 2016; Dichiara et al. 2016). To test whether precursor QPOs are common and the significance is related to the brightness of a precursor, we also investigated the correlation between the precursor’s Li-Ma significance and the p -value of a candidate QPO. The Pearson correlation coefficients for the precursors in SGRBs and LGRBs are 0.17 and 0.08, respectively, i.e., no clues are found for the common presence of QPOs in these precursors. Besides, we verified the robustness of the p -value estimation for the PDS method, that is, the percentage of samples smaller than a certain p -value is this p -value.

On the other hand, although some magnetar theories predict the possible existence of QPOs of tens of Hz in SGRB precursor (e.g. Sotani et al. 2007; Tews 2017; Zhang et al. 2022), the duration of the precursors of SGRBs is just about ~ 0.1 s (see Table.1), which means that only a few cycles of oscillations could possibly exist in a precursor, making the QPO search even more difficult. A definitive answer may come from sufficient statistics observed by more advanced detectors and higher detection signal to noise ratios, or a joined analysis using the light curves obtained by multiple GRB detectors, such as Fermi/GBM (Meegan et al. 2009), *Insight*-HXMT/HE (Zhang et al. 2020; Liu et al. 2020), Swift/BAT (Barthelmy et al. 2005), and GECAM (Li et al. 2021; Xiao et al. 2022c). Especially for detectors with similar energy response will be more advantageous, such as GECAM and GBM (Xiao et al. 2022d). Also can by combining with the information from theoretical models and the QPO evolution with time as a template in searching for QPOs (Dichiara et al. 2013).

In addition, for the Gaussian process method, we used the light curves of 1 ms time bin size to achieve a frequency search of up to 500 Hz. However, we find that there is an optimal time binsize with simulated data containing QPOs,

that is, the significance is lower when the time bin size is too small or too large. This may be similar to the phenomenon found in similar timing analysis (Ukwatta et al. 2010; Xiao et al. 2021; Xiao et al. 2022b), that is, when the time bin-size is too small, the statistical fluctuation in counts is large, and when the time bin is too large, the information in the light curves is lost. Therefore, we suggest that when possible QPO candidates exist (e.g. Significance obtained by PDS method is above 3σ), an appropriate time binsize should be chosen.

Although the QPO search in this work has only yielded negative results, an interesting product of the detailed search is the continuum properties of the PDS for the precursors and main emissions, which are also studied in this work for the first time. The study can help to constrain the energy dissipation in GRBs as a stochastic process and also the dissipation region (Titarchuk et al. 2007; Vaughan 2013; Guidorzi et al. 2016). Fig.5 shows the distribution of the power-law indices of PDS for the precursors and main emission of both SGRBs and LGRBs, and no significant difference is found, consistent with previous studies (Dichiara et al. 2013, 2016). The power-law indices are peaked at $\sim 5/3$, which is similar to that of the hydrodynamics in the Kolmogorov spectrum of velocity fluctuations within a medium characterized by a fully developed turbulence (Beloborodov et al. 1998).

In summary, we have performed systematic QPO search in the precursors of GRBs for the first time, which complements previous QPO studies. As well as reporting for the first time the distributions of the PDS of precursor and the relation with the main emission, which will contribute to further understanding of the physical mechanism of GRBs and their precursors (e.g. Narayan & Kumar 2009; Carballido & Lee 2011), as well as constraining the parameter space of the GRB internal shock model, such as the wind ejection properties determine the optical thickness of the wind in relativistic shells colliding with each other and dynamics (e.g. Rees & Meszaros 1994; Panaitescu et al. 1999).

ACKNOWLEDGMENTS

We thank the anonymous reviewer for a careful reading of our manuscript and insightful comments and suggestions. We acknowledge the public data from *Fermi*/GBM. The authors thank supports from the Strategic Priority Research Program on Space Science, the Chinese Academy of Sciences (Grant No. XDA15010100, XDA15360100, XDA15360102, XDA15360300, XDA15052700), the National Natural Science Foundation of China (Projects: 12061131007 and Grant No. 12173038). This work was partially supported by International Partnership Program of Chinese Academy of Sciences (Grant No.113111KYSB20190020). S. Xiao is grateful to W. Xiao, G. Q. Wang and J. H. Li for their useful comments.

REFERENCES

- Abbott, B. P., Abbott, R., Abbott, T., et al. 2017, *The Astrophysical Journal Letters*, 848, L13
- Barthelmy, S. D., Barbier, L. M., Cummings, J. R., et al. 2005, *Space Science Reviews*, 120, 143
- Beloborodov, A. M., Stern, B. E., & Svensson, R. 1998, *The Astrophysical Journal*, 508, L25
- Berger, E. 2014, *Annual review of Astronomy and Astrophysics*, 52, 43
- Burlon, D., Ghirlanda, G., Ghisellini, G., et al. 2008, *The Astrophysical Journal*, 685, L19
- Carballido, A., & Lee, W. H. 2011, *ApJL*, 727, L41, doi: [10.1088/2041-8205/727/2/L41](https://doi.org/10.1088/2041-8205/727/2/L41)
- Cenko, S., Butler, N., Ofek, E., et al. 2010, *The Astronomical Journal*, 140, 224
- Coppin, P., de Vries, K. D., & van Eijndhoven, N. 2020, *Physical Review D*, 102, 103014
- Dichiara, S., Guidorzi, C., Amati, L., Frontera, F., & Margutti, R. 2016, *Astronomy & Astrophysics*, 589, A97
- Dichiara, S., Guidorzi, C., Frontera, F., & Amati, L. 2013, *The Astrophysical Journal*, 777, 132
- Gao, H., Lei, W.-H., & Zhu, Z.-P. 2022, arXiv preprint arXiv:2205.05031
- Guidorzi, C., Dichiara, S., & Amati, L. 2016, *Astronomy & Astrophysics*, 589, A98
- Hansen, B. M., & Lyutikov, M. 2001, *Monthly Notices of the Royal Astronomical Society*, 322, 695
- Hu, Y.-D., Liang, E.-W., Xi, S.-Q., et al. 2014, *The Astrophysical Journal*, 789, 145
- Hübner, M., Huppenkothen, D., Lasky, P. D., & Inglis, A. R. 2022a, *The Astrophysical Journal Supplement Series*, 259, 32
- Hübner, M., Huppenkothen, D., Lasky, P. D., et al. 2022b, arXiv preprint arXiv:2205.12716
- Huppenkothen, D., Watts, A. L., Uttley, P., et al. 2013, *The Astrophysical Journal*, 768, 87
- Huppenkothen, D., Bachetti, M., Stevens, A. L., et al. 2019, *The Astrophysical Journal*, 881, 39
- Kruger, A. T., Lored, T. J., & Wasserman, I. 2002, *The Astrophysical Journal*, 576, 932
- Lewin, W. H., Van Paradijs, J., & Van der Klis, M. 1988, *Space Science Reviews*, 46, 273
- Li, L., & Mao, J. 2022, *The Astrophysical Journal*, 928, 152

- Li, L.-X., & Paczyński, B. 1998, *The Astrophysical Journal*, 507, L59
- Li, T.-P., & Ma, Y.-Q. 1983, *The Astrophysical Journal*, 272, 317
- Li, X., Wen, X., Xiong, S., et al. 2021, arXiv preprint arXiv:2112.04772
- Liu, C., Zhang, Y., Li, X., et al. 2020, *SCIENCE CHINA Physics, Mechanics & Astronomy*, 63, 1
- Lü, H.-J., Zhang, B., Liang, E.-W., Zhang, B.-B., & Sakamoto, T. 2014, *Monthly Notices of the Royal Astronomical Society*, 442, 1922
- Mangan, J., Dunwoody, R., Meegan, C., Team, F. G., et al. 2021, *GRB Coordinates Network*, 31210, 1
- Markwardt, C. B., Gavriil, F. P., Palmer, D. M., Baumgartner, W. H., & Barthelmy, S. D. 2009, *GRB Coordinates Network*, 9645, 1
- Meegan, C., Lichti, G., Bhat, P. N., et al. 2009, *ApJ*, 702, 791, doi: 10.1088/0004-637X/702/1/791
- Meegan, C., Lichti, G., Bhat, P., et al. 2009, *The Astrophysical Journal*, 702, 791
- Minaev, P. Y., & Pozanenko, A. 2017, *Astronomy Letters*, 43, 1
- Narayan, R., & Kumar, P. 2009, *Monthly Notices of the Royal Astronomical Society: Letters*, 394, L117
- Palenzuela, C., Lehner, L., Ponce, M., et al. 2013, *Physical review letters*, 111, 061105
- Panaitescu, A., Spada, M., & Mészáros, P. 1999, *ApJL*, 522, L105, doi: 10.1086/312230
- Rastinejad, J., Gompertz, B., Levan, A., et al. 2022, arXiv preprint arXiv:2204.10864
- Rees, M. J., & Meszaros, P. 1994, *ApJL*, 430, L93, doi: 10.1086/187446
- Sarin, N., & Lasky, P. D. 2021, *General Relativity and Gravitation*, 53, 1
- Sotani, H., Kokkotas, K., & Stergioulas, N. 2007, *Monthly Notices of the Royal Astronomical Society*, 375, 261
- Sridhar, N., Zrake, J., Metzger, B. D., Sironi, L., & Giannios, D. 2021, *Monthly Notices of the Royal Astronomical Society*, 501, 3184
- Stone, N., Loeb, A., & Berger, E. 2013, *Physical Review D*, 87, 084053
- Suvorov, A. G., Kuan, H.-J., & Kokkotas, K. D. 2022, arXiv preprint arXiv:2205.11112
- Suvorov, A. G., Kuan, H.-J., & Kokkotas, K. D. 2022, arXiv e-prints, arXiv:2205.11112. <https://arxiv.org/abs/2205.11112>
- Tarnopolski, M., & Marchenko, V. 2021, *The Astrophysical Journal*, 911, 20
- Tews, I. 2017, *Physical Review C*, 95, 015803
- Titarchuk, L., Shaposhnikov, N., & Arefiev, V. 2007, *The Astrophysical Journal*, 660, 556
- Troja, E., Rosswog, S., & Gehrels, N. 2010, *The Astrophysical Journal*, 723, 1711
- Troja, E., Fryer, C., O'Connor, B., et al. 2022, arXiv preprint arXiv:2209.03363
- Tsang, D., Read, J. S., Hinderer, T., Piro, A. L., & Bondarescu, R. 2012, *PhRvL*, 108, 011102, doi: 10.1103/PhysRevLett.108.011102
- Ukwatta, T., Stamatikos, M., Dhuga, K., et al. 2010, *The Astrophysical Journal*, 711, 1073
- Vaughan, S. 2005, *Astronomy & Astrophysics*, 431, 391
- Vaughan, S. 2010, *MNRAS*, 402, 307, doi: 10.1111/j.1365-2966.2009.15868.x
- Vaughan, S. 2013, *Philosophical Transactions of the Royal Society A: Mathematical, Physical and Engineering Sciences*, 371, 20110549
- Wang, J.-S., Peng, F.-K., Wu, K., & Dai, Z.-G. 2018, *The Astrophysical Journal*, 868, 19
- Wang, J.-S., Peng, Z.-K., Zou, J.-H., Zhang, B.-B., & Zhang, B. 2020, *The Astrophysical Journal Letters*, 902, L42
- Woosley, S., & Bloom, J. 2006, *Annu. Rev. Astron. Astrophys.*, 44, 507
- Wu, M.-R., Tamborra, I., Just, O., & Janka, H.-T. 2017, *Physical Review D*, 96, 123015
- Xiao, S., Xiong, S. L., Zhang, S. N., et al. 2021, *ApJ*, 920, 43, doi: 10.3847/1538-4357/ac1420
- Xiao, S., Zhang, Y.-Q., Zhu, Z.-P., et al. 2022a, arXiv preprint arXiv:2205.02186
- Xiao, S., Xiong, S.-L., Wang, Y., et al. 2022b, *The Astrophysical Journal Letters*, 924, L29
- Xiao, S., Liu, Y., Peng, W., et al. 2022c, *Monthly Notices of the Royal Astronomical Society*, 511, 964
- Xiao, S., Xiong, S.-L., Cai, C., et al. 2022d, *Monthly Notices of the Royal Astronomical Society*
- Yang, J., Zhang, B.-B., Ai, S., et al. 2022, arXiv preprint arXiv:2204.12771
- Zhang, S.-N., Li, T., Lu, F., et al. 2020, *SCIENCE CHINA Physics, Mechanics & Astronomy*, 63, 1
- Zhang, Z., Yi, S.-X., Zhang, S.-N., Xiong, S.-L., & Xiao, S. 2022, arXiv preprint arXiv:2207.12324
- Zhilyaev, B., & Dubinovska, D. 2009, *Astronomische Nachrichten: Astronomical Notes*, 330, 404
- Zhong, S.-Q., Dai, Z.-G., Cheng, J.-G., Lan, L., & Zhang, H.-M. 2019, *The Astrophysical Journal*, 884, 25

APPENDIX

Table S1. QPOs search for precursors in LGRBs using Power density spectrum.
The Tpre is from [Coppin et al. 2020](#).

Name	Tpre (s)	Li-Ma Significance (σ)	f_{PDS} (Hz)	p_{value} (PDS)
GRB 080723557	28.3	45.8	603	0.911
GRB 080807993	1.0	34.9	534	0.911
GRB 080816503	1.8	14.3	481	0.148
GRB 080818579	5.6	9.2	981	0.803
GRB 080830368	5.1	8.2	63	0.934
GRB 081003644	4.3	8.2	59	0.586
GRB 081121858	7.9	6.9	91	0.790
GRB 090101758	6.1	7.9	776	0.756
GRB 090113778	0.1	0.8	780	0.486
GRB 090117335	1.3	9.3	806	0.077
GRB 090131090	12.4	47.6	688	0.086
GRB 090309767	6.1	10.8	337	0.334
GRB 090419997	23.3	10.7	890	0.454
GRB 090425377	2.7	10.8	862	0.509
GRB 090502777	3.1	5.2	180	0.181
GRB 090610723	6.7	9.1	217	0.500
GRB 090618353	28.9	31.5	966	0.869
GRB 090810659	43.3	4.7	375	0.142
GRB 090811696	1.6	11.1	807	0.756
GRB 090814950	18.6	7.6	758	0.519
GRB 090820509	4.1	12.3	828	0.097
GRB 090907017	1.7	9.3	37	0.061
GRB 090929190	0.1	13.0	378	0.834
GRB 091109895	2.8	16.4	240	0.572
GRB 100116897	6.3	13.3	630	0.329
GRB 100130729	23.2	6.6	773	0.040
GRB 100204566	15.7	3.0	729	0.831
GRB 100323542	9.1	5.7	594	0.978
GRB 100517154	1.4	26.5	32	0.383
GRB 100619015	9.9	13.6	812	0.166
GRB 100625891	4.0	7.0	643	0.039
GRB 100709602	16.3	10.2	721	0.806
GRB 100718160	6.8	12.2	484	0.132
GRB 100923844	4.0	4.6	525	0.009
GRB 101224578	10.7	19.7	327	0.837
GRB 101227536	3.6	29.6	360	0.004
GRB 110102788	25.3	32.8	174	0.892
GRB 110227229	21.1	4.8	629	0.009
GRB 110428338	13.4	16.3	708	0.213
GRB 110528624	13.8	1.3	762	0.452
GRB 110725236	7.6	7.3	660	0.826

GRB 110729142	51.6	12.7	300	0.005
GRB 110825102	0.8	28.7	783	0.302
GRB 110903111	22.1	29.9	815	0.570
GRB 110904124	7.7	12.9	963	0.847
GRB 110909116	1.7	16.7	423	0.854
GRB 111010709	31.0	17.4	552	0.615
GRB 111015427	17.1	3.7	359	0.220
GRB 111230683	4.6	6.1	169	0.821
GRB 111230819	4.2	8.0	834	0.598
GRB 120308588	3.1	11.7	658	0.414
GRB 120319983	5.6	7.4	272	0.071
GRB 120412920	5.5	25.1	598	0.743
GRB 120504945	0.8	7.9	75	0.399
GRB 120530121	8.0	22.0	506	0.884
GRB 120611108	6.6	5.9	460	0.830
GRB 120710100	4.9	9.3	76	0.764
GRB 120711115	4.8	9.8	88	0.249
GRB 120716712	5.4	18.7	726	0.850
GRB 120819048	1.6	6.9	308	0.748
GRB 121005340	38.8	5.7	263	0.774
GRB 121029350	8.8	13.0	177	0.482
GRB 121031949	38.5	9.8	814	0.334
GRB 121113544	31.7	18.6	461	0.447
GRB 121125356	20.3	9.1	740	0.110
GRB 121217313	65.8	4.0	256	0.450
GRB 130104721	3.9	17.7	167	0.692
GRB 130106995	17.6	16.0	841	0.914
GRB 130208684	5.1	10.0	896	0.651
GRB 130209961	4.6	33.2	678	0.892
GRB 130219775	20.3	8.3	545	0.093
GRB 130310840	1.2	9.9	747	0.446
GRB 130318456	6.9	12.8	881	0.675
GRB 130320560	42.1	9.2	453	0.884
GRB 130404840	8.4	34.4	662	0.182
GRB 130418844	16.5	10.2	624	0.284
GRB 130623130	1.8	8.2	280	0.877
GRB 130720582	115.4	23.7	341	0.771
GRB 130813791	1.7	11.1	939	0.496
GRB 130815660	6.9	20.0	551	0.156
GRB 130818941	8.7	14.8	436	0.062
GRB 131014513	2.1	8.5	741	0.290
GRB 131108024	1.8	7.4	893	0.330
GRB 140104731	1.5	15.6	620	0.172
GRB 140108721	11.6	31.1	533	0.674
GRB 140126815	14.1	5.0	498	0.043
GRB 140304849	30.7	7.8	936	0.081
GRB 140329295	0.6	65.6	422	0.179
GRB 140404030	7.7	6.8	511	0.172
GRB 140512814	11.8	13.4	378	0.680

GRB 140621827	0.7	35.2	928	0.666
GRB 140628704	4.9	4.6	241	0.201
GRB 140709051	5.7	7.0	772	0.600
GRB 140714268	27.5	6.1	807	0.918
GRB 140716436	2.2	18.4	637	0.260
GRB 140818229	10.2	10.5	352	0.852
GRB 140824606	12.9	12.3	26	0.382
GRB 140825328	3.2	11.3	353	0.687
GRB 140917512	3.9	13.1	788	0.904
GRB 141029134	6.9	15.1	891	0.009
GRB 141102536	0.1	13.2	971	0.923
GRB 150126868	13.0	10.3	420	0.454
GRB 150127398	5.7	43.9	227	0.884
GRB 150226545	16.2	5.6	194	0.542
GRB 150330828	11.5	55.3	440	0.776
GRB 150506398	27.8	0.6	96	0.962
GRB 150508945	15.7	9.0	888	0.816
GRB 150512432	20.2	10.1	975	0.579
GRB 150522433	7.8	7.1	217	0.753
GRB 150523396	19.7	26.4	648	0.041
GRB 150702998	2.5	25.1	960	0.470
GRB 150703149	0.0	0.2	933	0.193
GRB 150830128	14.0	4.3	797	0.099
GRB 151027166	40.6	10.7	440	0.739
GRB 151030999	17.7	22.1	147	0.456
GRB 160131174	44.0	5.1	626	0.282
GRB 160201883	1.0	9.3	395	0.979
GRB 160215773	44.6	10.6	352	0.463
GRB 160219673	12.5	10.5	470	0.951
GRB 160223072	10.5	9.8	204	0.737
GRB 160225809	23.2	12.8	602	0.040
GRB 160512199	9.4	7.4	558	0.929
GRB 160519012	17.1	3.4	489	0.083
GRB 160523919	5.4	10.4	300	0.861
GRB 160625945	2.4	46.1	236	0.859
GRB 160724444	1.8	8.4	720	0.957
GRB 160821857	31.8	14.5	728	0.232
GRB 160825799	0.6	10.2	397	0.096
GRB 160908136	6.8	7.9	964	0.401
GRB 160912521	5.2	11.3	904	0.006
GRB 160919613	0.8	8.0	299	0.812
GRB 161105417	12.7	13.2	387	0.021
GRB 161111197	11.1	7.3	170	0.692
GRB 161117066	77.0	17.5	316	0.946
GRB 161119633	7.7	5.7	163	0.942
GRB 170109137	6.4	7.8	178	0.786
GRB 170115662	18.6	11.4	538	0.344
GRB 170209048	8.2	24.6	562	0.763
GRB 170302719	12.3	6.1	181	0.283

GRB 170323775	12.7	8.5	676	0.496
GRB 170402961	0.2	12.2	156	0.905
GRB 170416583	12.5	28.6	317	0.521
GRB 170514152	0.7	15.9	90	0.804
GRB 170514180	35.9	15.3	832	0.904
GRB 170830069	6.0	6.7	824	0.200
GRB 170831179	6.3	10.4	307	0.054
GRB 170923188	1.0	11.7	943	0.852
GRB 171004857	1.4	7.3	77	0.908
GRB 171102107	10.4	15.2	271	0.718
GRB 171112868	9.5	10.2	675	0.366
GRB 171120556	4.2	67.9	501	0.211
GRB 171211844	12.4	15.3	397	0.036
GRB 180307073	23.3	9.8	698	0.624
GRB 180411519	26.7	13.0	642	0.366
GRB 180416340	10.3	29.6	95	0.723
GRB 180618724	26.2	5.4	757	0.699
GRB 180620354	5.9	9.4	265	0.886
GRB 180710062	13.5	4.3	802	0.556
GRB 180720598	10.0	7.1	136	0.182
GRB 180728728	10.0	11.8	512	0.801
GRB 180822423	2.8	18.5	415	0.558
GRB 180906988	1.0	13.7	842	0.088
GRB 180929453	0.6	9.6	725	0.494
GRB 181008877	27.9	6.9	630	0.909
GRB 181119606	1.8	49.5	232	0.622
GRB 181122381	0.3	18.4	933	0.468
GRB 181203880	0.9	9.1	821	0.389
GRB 181222279	40.8	28.9	155	0.790
GRB 190114873	1.5	6.4	361	0.182
GRB 190228973	8.0	10.5	947	0.570
GRB 190310398	4.1	17.1	258	0.968
GRB 190326314	2.1	18.8	685	0.691
GRB 190610750	1.2	20.5	835	0.549
GRB 190611950	20.1	44.2	920	0.610
GRB 190719624	1.6	27.5	751	0.714
GRB 190806675	1.2	16.7	627	0.184
GRB 190828542	38.5	2.2	979	0.927
GRB 190829830	5.6	21.9	767	0.791
GRB 190901890	20.0	1.1	608	0.620
GRB 190930400	40.3	7.1	832	0.259
GRB 191019970	29.8	28.8	768	0.077
GRB 191026350	4.1	6.0	896	0.050
GRB 191031025	10.4	6.9	774	0.133
GRB 191101895	1.9	6.8	396	0.027
GRB 191111364	16.4	6.5	647	0.133
